Direct-Channel Description of the Reactions $\pi^- p \to \eta n$ and $\pi^- p \to \pi^0 n$ at High Energy*

Jerome S. Danburg
Physics Department, Brookhaven National Laboratory, Upton, New York 11973
(Received 13 January 1971)

Amplitudes made up only of direct-channel resonance contributions are constructed in accordance with a simple model to fit the high-energy data for the reactions $\pi^- p \to \eta n$ and $\pi^- p \to \pi^0 n$. A good fit is obtained for the differential cross section, total cross section, and the (sparse) polarization data at high energy for $\pi^- p \to \eta n$. For the charge-exchange reaction, the fits to the total cross section, the polarization, and the forward peak of the differential cross section are satisfactory; a simple extension of the model is shown to account in a rough way for the secondary peak in the differential cross section and its disappearance with increasing energy.

INTRODUCTION

Recently there has been much discussion of the way in which the peripheral behavior of two-body scattering is related to direct-channel resonances. Schmid[1] has shown, using a partial-wave analysis, that a Regge amplitude for πN charge-exchange scattering at high energy exhibits typical resonance phase behavior, i.e., generates loops in the Argand diagram for the low partial waves at low momentum (1–2 GeV/c). Subsequently, Kugler[2] examined the high-s partial-wave decomposition of a Regge amplitude and concluded that resonance-like phase behavior occurs in the highest contributing partial waves even at high energy. Harari[3,4] has also discussed the possible role of resonances in peripheral-scattering processes.

A number of papers have since been written which propose specific direct-channel resonance models for peripheral-scattering processes. Shapiro[5] has proposed a Veneziano-type resonance model. Dikmen[6,7] has used a combination of the Pomeranchuk Regge trajectory and direct-channel resonances to fit elastic pion-nucleon and kaon-nucleon scattering data. Recently Crittenden *et al.*[8] have fitted the backward $\pi^+ p$ elastic differential cross section up to 5 GeV/c using only direct-channel resonance contributions. It is noted that even before the importance of direct-channel resonances was stressed in the framework of duality, Hoff[9] and Dikmen[10] had pointed out that for $\pi^- p$ elastic scattering the features of the forward peak up to beam momenta of 2.5 GeV/c [9] and of the backward peak up to 5 GeV/c [10] can be adequately accounted for using direct-channel resonances. The approach outlined in the present paper differs from those given in the above references; a comparison of these models with the present paper will be made following the presentation of the model.

Here we wish to examine whether an amplitude built up *entirely* from ordinary direct-channel resonance contributions can account directly for the behavior of inelastic two-body reactions not only near threshold, but at high energies as well. We consider two-body scattering with a 0^- meson and a $\frac{1}{2}^+$ baryon in both the initial and final states. It will be shown, using simple and plausible physical assumptions, how an amplitude constructed using direct-channel resonances alone can describe many features of inelastic peripheral reactions at all energies.

DESCRIPTION OF THE AMPLITUDE

Our object is to construct, using direct-channel resonances only, an amplitude which yields a forward peak having a width (in t) which is constant with energy. This behavior is, in some approximation, a characteristic of all forward two-body differential cross sections. To construct an amplitude with this behavior, we proceed by analogy to a classical diffraction amplitude for momentum k and diffraction radius R; this amplitude is

$$A \propto \sum_{l=0}^{kR} (2l+1) P_l(\cos\theta). \tag{1}$$

The important features of this amplitude for the present discussion are that (a) all partial waves from 0 to the highest value are present, (b) all the partial waves have the same phase, (c) each partial wave contributes equally, that is, each P_l enters with a weight $\propto l$, and (d) the sum cuts off at the partial wave $L = kR$. The t distribution resulting from such an amplitude has a constant width $\propto R^{-2}$.

Now the spin-nonflip and spin-flip amplitudes

for the meson-baryon scattering process

$$M(0^-)+B(\tfrac{1}{2}^+)\to M'(0^-)+B'(\tfrac{1}{2}^+),$$

e.g., for πN charge exchange or $\pi N\to\eta N$ scattering, are

$$f^+=\sum_l (l+1)T_l^+P_l(x), \tag{2a}$$

$$g^+=\sum_l T_l^+\sin\theta\,\frac{dP_l(x)}{dx} \tag{2b}$$

for $J=l+\frac{1}{2}$ (J is the total angular momentum) and

$$f^-=\sum_l l\,T_l^-P_l(x), \tag{3a}$$

$$g^-=-\sum_l T_l^-\sin\theta\,\frac{dP_l(x)}{dx} \tag{3b}$$

for $J=l-\frac{1}{2}$. Here $x=\cos\theta$, and f and g denote, respectively, the spin-nonflip and spin-flip amplitudes. Now we construct a peripheral amplitude from a series of direct-channel resonances satisfying either $J=l+\frac{1}{2}$ or $J=l-\frac{1}{2}$. In order to satisfy the above property (a) of a diffraction amplitude, we require that *every* partial wave contain a resonance (not just the even or odd partial waves). Of course, each partial wave may contain more than one resonance, and this situation will be discussed below in connection with the fits performed, but for the present discussion we consider only one resonance in each partial wave. One expects, because of angular momentum barriers, no contribution from resonances in partial waves l such that the resonance mass E_l is much greater than the c.m. energy $E=\sqrt{s}$; i.e., the sums in Eqs. (2) and (3) are expected to cut off when $E_l\approx E$. Thus if we set, for high energy at least,

$$E_l\approx\alpha l, \tag{4}$$

the sums will cut off at

$$L\approx E/\alpha\approx 2k/\alpha, \tag{5}$$

in accordance with property (d) of a diffraction amplitude, and we find by comparison with Eq. (1) that the diffraction radius is $R=2/\alpha$. We have used $k\cong\frac{1}{2}E$ at high energy. Let all resonances enter with the same phase, and assume a simple Breit-Wigner line shape, so that

$$T_l=\frac{\Gamma_{if}}{E_l-E-\frac{1}{2}i\Gamma_l^{\rm tot}}. \tag{6}$$

Γ_{if} is the square root of $\Gamma_i\Gamma_f$, where Γ_i and Γ_f are the couplings to the initial- and final-state channels. Let each resonance contribute to the amplitude even when E is far from E_l, so that Eq. (6) is valid for all E, but let Γ_{if} (for which we have suppressed a subscript l) be damped by an angular momentum barrier function for all l such that $E<E_l$.

It is seen from Eq. (6) and the expressions (2) and (3) that for l such that $E_l<<E$, the nonflip partial-wave amplitude is

$$f_l\propto -1/E,\quad l<<E/\alpha \tag{7}$$

whereas for the last wave in the sum,

$$f_L\propto 2i/\Gamma_L^{\rm tot},\quad L=E/\alpha. \tag{8}$$

In order to make the contributions of the highest and lowest partial waves as nearly equal as possible, in accordance with the above property (c) of a diffraction amplitude, we require

$$\Gamma_L^{\rm tot}\propto E=E_L,\quad \text{i.e.,}\quad \Gamma_l\propto E_l. \tag{9}$$

Having done this, we note that the contributing partial waves do not all have the same phase, but have a distribution in phase between π and $\frac{1}{2}\pi$.

The total reaction cross section obtained from the amplitude constructed above is

$$\sigma^{\pm}=\frac{1}{s}\frac{k_f}{k_i}\left(\sum_{l=0}^{E/\alpha}2W_l^{\pm}\,|A_l^{\rm BW}|^2\right), \tag{10}$$

where $W_l^+=l+1$, $W_l^-=l$; k_i and k_f are the initial- and final-state c.m. momenta; and $A_l^{\rm BW}$ is the Breit-Wigner amplitude (6). Taking

$$E_l=\alpha l,\quad \Gamma_l^{\rm tot}=\beta l, \tag{11}$$

and approximating the sum by an integral (in performing the integration, the effect of the angular momentum barrier functions on the contributing partial waves is ignored for simplicity) gives a constant for the terms in brackets in Eq. (10). This means that for the total cross section to fall with s as s^{-n}, where for typical inelastic reactions[11] n lies between 1.5 and 3, an additional dependence of roughly E^{-1} must be inserted into the two-body width Γ_{if} of Eq. (6). This dependence will be different for different final states, since Morrison has noted[11] that reactions like $\pi N\to KY$ and $KN\to\pi Y$ generally fall off faster with energy than $\pi N\to\pi N'$ and $KN\to KN'$.

A few further points about such an amplitude are of interest:

(1) Equations (2) and (3) specify the exact relative amounts of spin-flip and spin-nonflip amplitudes; in fact, the f and g amplitudes contribute almost equally to the cross section at high energy for both the $J=l+\frac{1}{2}$ and the $J=l-\frac{1}{2}$ trajectories. In order to obtain a different ratio of spin-flip to spin-nonflip amplitude, it is then necessary to invoke interference between at least two direct-channel trajectories or even between a $J=l+\frac{1}{2}$ and a $J=l-\frac{1}{2}$ trajectory (if both exist). This is a difficulty which does not arise in a Regge fit, where the spin-flip and -nonflip amplitudes are parametrized separately.

(2) Prominent dips will occur at fixed t values in the spin-flip and -nonflip differential cross sections *separately* if, in Eq. (11), $\beta^2/4 \ll \alpha^2$. In this case the partial waves near the last (Lth) wave dominate the amplitude, and the first zero of P_L occurs at a scattering cosine proportional to $1/L^2 = \alpha^2/t_{\max}$ from the forward direction, a fact noted by Dolen, Horn, and Schmid[12] and by Harari.[4] However, since $f_L \propto P_L$ and $g_L \propto P_L'$, the dips in the spin-flip amplitude will be shifted with respect to those in the spin-nonflip amplitude. Thus barring cancellation of one or the other amplitude as in point (1) above, a smooth differential cross section will result. This situation is illustrated clearly in Fig. 1, where the spin-flip and -nonflip differential cross sections at two incident momenta are plotted separately for $\beta = 2\alpha$ and for $\beta = 0.37\alpha$.

(3) Barring cancellation of either the spin-flip or -nonflip term by interference of two or more direct-channel trajectories, the final-state nucleon polarization is in general nonzero.

(4) The diffractionlike peak resulting from the pure-resonance amplitude constructed here can be made to shrink or expand with energy by making the resonance spacing become smaller or greater with energy, but this will cause the dips noted in point (2) to move as well. The amplitude given here exhibits some residual shrinkage even for the uniform resonance spacing given in Eq. (12) below. This is because the cutoff value of L in the partial-wave sum does not approach the value given by Eq. (5) until the c.m. energy is large compared to about 1 GeV, which means that the residual shrinkage persists up to beam momenta of about 15 or 20 GeV/c. This is apparent in Fig. 1.

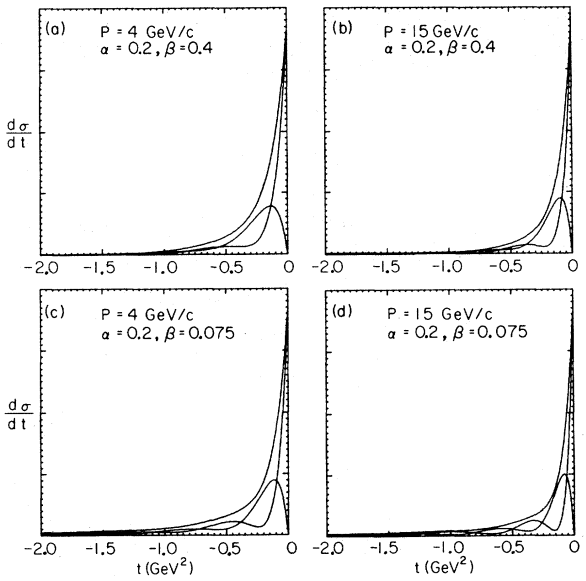

FIG. 1. Differential cross sections using $\pi N \to \pi N$ kinematics for the example discussed in the text; α and β are in GeV. The spin-flip and spin-nonflip contributions, and their sum (upper curve) are plotted separately.

(5) The amplitude constructed here is for the scattering of a 0^- meson and a $\frac{1}{2}^+$ baryon; if the interacting particles have different spins, a different amplitude must be examined. This point raises the crucial question of whether such a direct-channel description can account for the spin alignment of the final-state particles in the case of arbitrary spins.

(6) A pure-resonance amplitude does not at first sight seem applicable to channels such as $K^+n \to K^0p$, where there is no (obvious) resonance structure. However, in exotic channels such as this one the resonances, if they are present, might differ from those in nonexotic channels by being broader or by having smaller interaction radii (see Ref. 13). These effects would make such exotic resonances difficult to observe. It is interesting to note that in his discussion of K^+p elastic scattering, Dikmen[7] suggests that a contribution from Z^* resonances is required by his fits.

(7) We note also that for elastic processes, for which the cross sections approach constant values at high energy, the contribution of simple diffraction scattering must be added to that part assumed to come from resonances.

Before proceeding to the fits, we display some curves obtained using a simple amplitude like the one constructed above. Figure 1 shows differential cross sections obtained using $\pi N \to \pi N$ kinematics for a direct-channel trajectory with $J = l + \frac{1}{2}$ and

$$E_l = 1.30 + 0.2l \text{ GeV}, \quad \Gamma_l^{\text{tot}} = (0.10 \text{ GeV}) + \beta l, \tag{12}$$

where $\beta = 0.400 \text{ GeV} = 2\alpha$ in Figs. 1(a) and 1(b), and $\beta = 0.075 \text{ GeV} = 0.37\alpha$ in Figs. 1(c) and 1(d). For each l the angular momentum barrier factors in Γ_{if} are approximated by the function[13]

$$B_l = \frac{(k/k_l)^{2l+1}}{1 + (k/k_l)^{2l+1}}, \tag{13}$$

where k is the c.m. momentum and k_l is the c.m. momentum at the resonance mass. The barrier factor (13) produces a very sharp cutoff at the partial wave L such that $E_L = E$, but in the computer calculations the sums were carried past this value. The starting values of the resonance mass (1.3 GeV) and width (100 MeV) are reasonable ones for πN scattering; the resonance spacing $\alpha = 0.2$ GeV is chosen to give a differential cross-section width of about 0.75 GeV^2 in t, which is typical for two-body reactions. At low energies this parametrization of the resonance masses and widths is of course not

meant to be an exact description of the baryon spectrum; we will return to this point in the discussion of the fits below. The incident-momentum values used in the example of Fig. 1 were chosen to show how pronounced the peripheral peak is even at moderately low momentum (4 GeV/c), and to demonstrate the asymptotic t behavior at 15 GeV/c.

METHOD USED IN THE FITS

The high-energy data for the reactions $\pi^- p \to \eta n$ and $\pi^- p \to \pi^0 n$ are fitted using simple amplitudes constructed as described above. Before proceeding to the particulars of the fits, we note the basic method by which the fits will be performed: The data will be described in both cases using trajectories of direct-channel resonances satisfying

$$E_l = E_0 + \alpha l, \quad \Gamma_l^{\text{tot}} = \Gamma_0^{\text{tot}} + \beta l, \tag{14}$$

where l is the meson-baryon orbital angular momentum. The total angular momentum J of a trajectory will be assumed to satisfy either $J = l + \frac{1}{2}$ or $J = l - \frac{1}{2}$ [equivalently, the parity is given by $P = (-)^{J \pm 1/2}$]; the amplitudes for each type of trajectory are given by Eqs. (2) and (3). Each resonance is described by the simple Breit-Wigner line shape given in Eq. (6). The choice of this line shape is of course arbitrary; it is used because of the simplicity of the results it yields, as described above. The initial- to final-state coupling Γ_{if} is assumed, at a given energy, to be the same for all resonances and is assumed to have the energy dependence

$$\Gamma_{if} = \Gamma_{if,0}(E/E_0)^{-\gamma}. \tag{15}$$

The total width Γ_l^{tot} of each resonance is taken as constant.

The reactions $\pi^- p \to \eta n$ and $\pi^- p \to \pi^0 n$ are both characterized by the dominance of the spin-flip amplitude over the spin-nonflip amplitude over the entire range of energies at which they have been measured. Since a single direct-channel trajectory yields almost equal amounts of spin-flip and -nonflip contributions, it is then necessary to assume that most of the spin-nonflip contribution is cancelled through the interference of two or more direct-channel trajectories. In fitting both reactions the simplest possibility will be assumed: that two trajectories with similar energy spectra contribute coherently to each reaction. It will further be assumed that one of the two contributing trajectories satisfies $J = l + \frac{1}{2}$ and that the other satisfies $J = l - \frac{1}{2}$, and that both trajectories have identical mass and width spectra, as given by Eq. (14). Since a $J = l + \frac{1}{2}$ trajectory has the spin-flip and -nonflip amplitudes entering with the same sign, whereas a $J = l - \frac{1}{2}$ trajectory has the spin-flip and -nonflip amplitudes entering with opposite signs [see Eqs. (2) and (3)], it will simply be assumed that the two trajectories (with $J = l \pm \frac{1}{2}$) contribute with comparable strengths but opposite signs to the amplitude for each reaction. One could also perform fits by varying both the amounts *and* the relative phase of the two trajectories, but for simplicity the relative phase of the two amplitudes was fixed at 180°. The procedure adopted yields in a simple way the dominance of the spin-flip over the spin-nonflip amplitude.

THE REACTION $\pi^- p \to \eta n$

Reference 14 contains a list of experimental papers on this reaction. First the differential cross-section data from this reaction were fitted; the data are those measured by Danburg[14] in the charge-symmetric reaction at beam momenta between 1.1 and 2.4 GeV/c, and the data of Guisan *et al.*[15] for beam momenta between 3 and 18 GeV/c. It was assumed, as explained above, that two direct-channel trajectories with $J = l \pm \frac{1}{2}$ dominate the reaction at high energy; these were taken to be described by

$$E_l = (1530\ \text{MeV}) + \alpha l, \quad \Gamma_l^{\text{tot}} = (80\ \text{MeV}) + \beta l. \tag{16}$$

The coupling between the initial and final states was assumed to have the same energy dependence for both trajectories, as given by Eq. (15), but the strengths were allowed to differ by an over-all factor. The two trajectories were assumed to contribute to the over-all amplitude with opposite signs. Note that the starting values in the trajectory spectra of Eq. (16) are chosen to coincide with the mass and width of the $N(1530)$ S_{11} resonance just above threshold for this reaction. If one attempts, using the Particle Data Group tables[16] to correlate the assumed direct-channel trajectories with the observed resonances which couple to both the πN and ηN channels, one might guess that the first two members of a $J = l + \frac{1}{2}$ trajectory are

$$J^P = \tfrac{1}{2}^-: \quad N(\sim 1530), \quad \Gamma^{\text{tot}} = 50\text{–}160\ \text{MeV}, \quad \Gamma(\pi N \to \eta N) = 25\text{–}80\ \text{MeV};$$

$$J^P = \tfrac{3}{2}^+: \quad N(\sim 1860), \quad \Gamma^{\text{tot}} = 310\text{–}450\ \text{MeV}, \quad \Gamma(\pi N \to \eta N) = 30\text{–}45\ \text{MeV},$$

whereas the first member of a $J = l - \frac{1}{2}$ trajectory might be

$$J^P = \tfrac{1}{2}^+: \quad N(\sim 1780), \quad \Gamma^{\text{tot}} = 270\text{–}450\ \text{MeV}, \quad \Gamma(\pi N \to \eta N) = 50\text{–}80\ \text{MeV}.$$

These assignments ignore the S_{11} resonance $N(\sim 1700)$ which decays into ηN; this is a slight difficulty. One could of course assume that some of the prominent low-mass resonances do not lie on

trajectories with $E_l \propto l$, as is proposed here, or one could assume that there are more than two contributing trajectories. At any rate, the starting values of resonance mass and width, given in Eq. (16), are reasonable ones for this problem.

A least-squares fitting procedure was employed to fit the differential cross sections; the parameters α and β in Eq. (16), and the relative amounts of the $J = l + \frac{1}{2}$ and $J = l - \frac{1}{2}$ trajectories were varied. The line shape given in Eq. (6), with the angular momentum barrier factor given in Eq. (13) were used. Note that with this barrier function, the radius of interaction for each resonance is $\rho_l = 1/k_l$, where k_l is the final-state c.m. momentum at the resonance mass. A more general form, as discussed above, is

$$\rho_l = r/k_l. \tag{17}$$

Thus the solution obtained is not unique because it is the ratio r/α that determines how many partial waves enter each amplitude. The fits performed here yield a value of α obtained with $r = 1$, but r can be changed by a factor close to 1 and essentially the same results are obtained by multiplying α by the same factor. It has been noted that if $\beta < 2\alpha$, prominent dips occur in the differential cross section; furthermore in this case the amplitude yields a differential cross section which has a substantial high-t tail, since the highest partial waves dominate the amplitude. These remarks can be clarified by reference to Fig. 1. Since the differential cross section for $\pi N \to \eta N$ is confined to a forward peak, the best fits were obtained with $\beta \geq 2\alpha$. The fits were not very sensitive to values of β greater than 2α, so the results given here are for $\beta = 2\alpha$. The least-squares procedure yielded the best fit when $\alpha = 200$ MeV ($\pm 10\%$) is the resonance spacing. The differential cross sections can be adequately described by having the relative contributions of the $J = l \pm \frac{1}{2}$ trajectories anywhere between a ratio of 1 and 2; for relative amounts between these limits the spin-flip contribution is much larger than that of the spin-nonflip amplitude. The

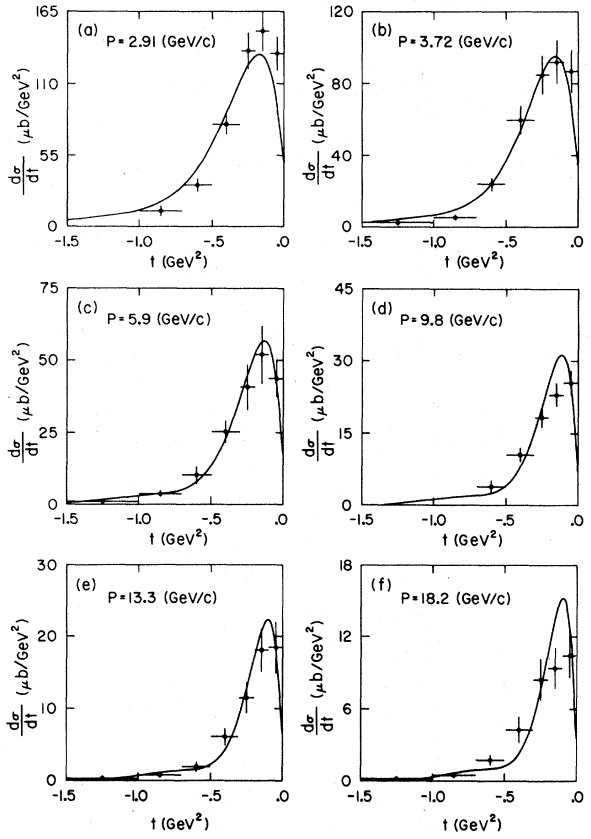

FIG. 2. Differential cross section for $\pi^- p \to \eta n$, $\eta \to \gamma\gamma$, measured by Guisan *et al.* (Ref. 15) at six incident beam momenta. The curves are from the fit described in the text; each curve is normalized to have the same area as the experimental points.

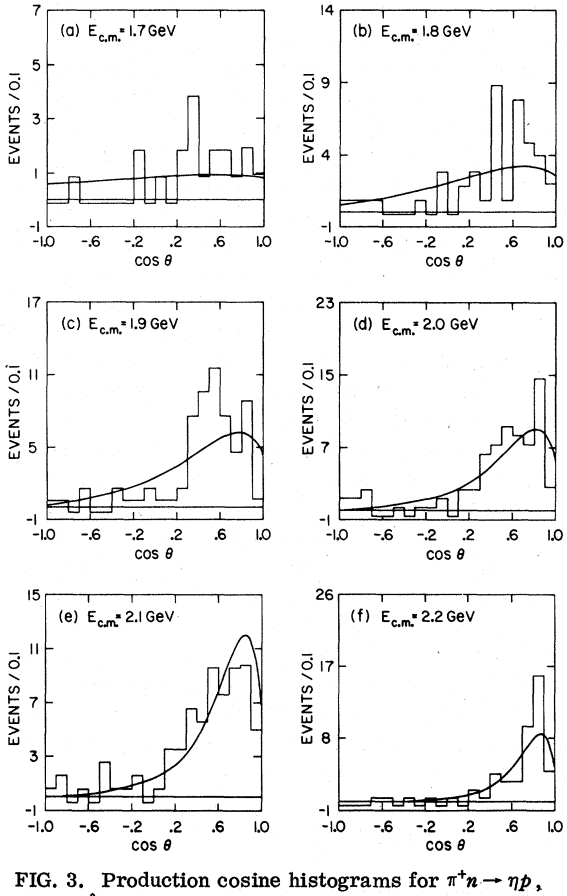

FIG. 3. Production cosine histograms for $\pi^+ n \to \eta p$, $\eta \to \pi^+\pi^-\pi^0$, measured by Danburg (Ref. 14) in six c.m. energy intervals, each of which is 100-MeV wide and centered at the value given. The curves are from the fit described in the text; each curve is normalized to have the same area as the experimental histogram.

polarization data for this reaction are used to determine more exactly the amounts of the two assumed direct-channel trajectories. The available high-energy polarization data for this reaction are from Drobnis *et al.*[17] and Bonamy *et al.*[18] Although very few polarization data have been measured, it appears that a small (~15%) polarization for $|t| < 0.3$ GeV^2 persists up to $p_{\text{lab}} = 11$ GeV/c. A satisfactory fit to the polarization data was obtained with

$$A = 1.4A^+ - A^-. \tag{18}$$

Here A is the amplitude for $\pi N \to \eta N$, and $A^\pm$ is the amplitude for the $J = l \pm \frac{1}{2}$ trajectory, as given in Eqs. (2) and (3). Finally the power of the c.m. energy with which the cross-channel coupling falls off was determined by a fit to the high-energy data to be about $\gamma = 0.7$.

Summarizing, the results of the fit to $\pi N \to \eta N$ are: $\alpha = 200$ MeV (±10%) is the resonance-mass spacing, with the radius of interaction given by Eq. (17) where $r = 1$, and $\beta = 400$ MeV is the increase in resonance width for $\Delta l = 1$. The amounts of the assumed $J = l \pm \frac{1}{2}$ trajectories are given by Eq. (18), and $\gamma = 0.7$ is the exponent in Eq. (15).

Figure 2 shows the differential cross sections measured by Guisan *et al.*[15] at high energy, and Fig. 3 shows those of Danburg[14] at lower energies. The curves are from the fits described above; in all cases the curves are normalized to the area of the experimental points. In Fig. 2 it is seen that the measured differential cross section shrinks noticeably between 3 and 18 GeV/c. This narrowing of the forward peak is well described by the curves; this is the residual shrinkage discussed in the above-stated property (4) of the amplitude used here. The amplitude yields essentially no more shrinkage at incident beam momenta above 20 GeV/c; measurements of the differential cross section at higher momenta will therefore provide a test of the simple form of resonance amplitude used here. Figure 4 shows the polarization data of Drobnis *et al.*[17] and Bonamy *et al.*[18] along with the results of the fit. Figure 5 is a plot of the total cross-section data of Bulos *et al.*,[19] Danburg,[14] and Guisan *et al.*[15] The curve is the result of the fit; it is normalized to pass through the data point at $P = 3.72$ GeV/c. Note that the measured total cross section is substantially underestimated at low momentum.

THE REACTION $\pi^- p \to \pi^0 n$

The differential cross-section data of Sonderegger *et al.*[20] at beam momenta between 3 and 18 GeV/c were used to fit this reaction. The presence in the differential cross section of a secondary peak which disappears with increasing energy is a feature which cannot be described in a simple way by an amplitude of the type described here. This is because the present amplitude has an asymptotic fixed-t behavior. Nevertheless, the shape of the forward peak in the differential cross

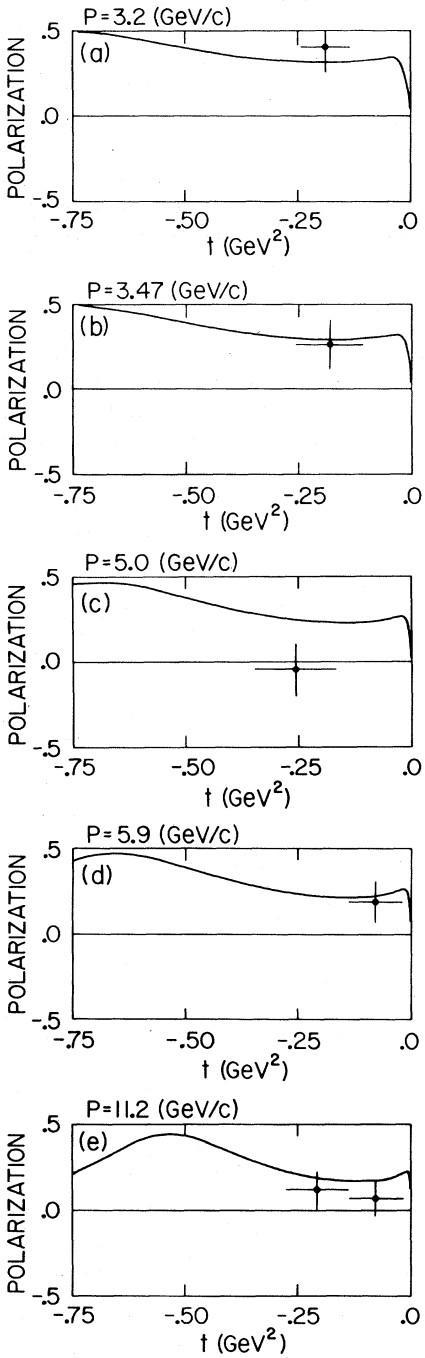

FIG. 4. Polarization in the reaction $\pi^- p \to \eta n$. (a)–(c) from Drobnis *et al.*, Ref. 17; (d)–(e) from Bonamy *et al.*, Ref. 18. The curves are from the fit described in the text.

section changes little from 3 to 18 GeV/c, and we first restrict the fit to the data in the forward peak.

The mass and width spectra of the two assumed trajectories were assumed to have the high-energy behavior

$$E_l = (1200\ \text{MeV}) + \alpha l, \quad \Gamma_l^{\text{tot}} = (100\ \text{MeV}) + \beta l. \tag{19}$$

The fits were, as in the case of η production, best for $\beta \geq 2\alpha$, and $\beta = 2\alpha$ was used. Because the forward peak is narrower for the charge-exchange reaction than for $\pi N \to \eta N$, a closer resonance spacing (~150 MeV) is obtained for this reaction when $r = 1$ in Eq. (17). In order to show that both the η production and the charge-exchange reactions could proceed via similar direct-channel trajectories, we have arbitrarily selected $\alpha = 200$ MeV as was obtained for $\pi N \to \eta N$. The best fit was then obtained with $r = 1.33$ (±10%).

At this point we indicate which low-mass resonances might lie on the assumed dominant two trajectories. We note the well-known fact that the πN channel seems to couple more strongly to $I = \frac{3}{2}$ resonances with $J = l + \frac{1}{2}$ than to those with $J = l - \frac{1}{2}$, whereas $I = \frac{1}{2}$ resonances with $J = l - \frac{1}{2}$ couple more strongly to πN than those with $J = l + \frac{1}{2}$. We will thus note only a few $I = \frac{3}{2}$ resonances with $J = l + \frac{1}{2}$ and some $I = \frac{1}{2}$ resonances with $J = l - \frac{1}{2}$ as candidates for the two assumed dominant direct-channel trajectories. For $J = l + \frac{1}{2}$ one might choose

$J^P = \frac{1}{2}^-$: no choice with mass < 1236 MeV;

$J^P = \frac{3}{2}^+$: $\Delta(1236)$, $\Gamma^{\text{tot}} = 120$ MeV, $\Gamma(\pi N \to \pi N) = 120$ MeV;

$J^P = \frac{5}{2}^-$: $\Delta(\sim 1954)$, $\Gamma^{\text{tot}} \approx 300$ MeV, $\Gamma(\pi N \to \pi N) \approx 50$ MeV (Ref. 21);

$J^P = \frac{7}{2}^+$: $\Delta(\sim 1950)$, $\Gamma^{\text{tot}} = 140$–$220$ MeV, $\Gamma(\pi N \to \pi N) = 60$–$100$ MeV;

$J^P = \frac{9}{2}^-$: no candidate;

$J^P = \frac{11}{2}^+$: $\Delta(2420)$, $\Gamma^{\text{tot}} \approx 310$ MeV, $\Gamma(\pi N \to \pi N) \approx 35$ MeV.

For $J = l - \frac{1}{2}$ one might take

$J^P = \frac{1}{2}^+$: $N(\sim 1470)$, $\Gamma^{\text{tot}} = 200$–$400$ MeV, $\Gamma(\pi N \to \pi N) = 120$–$240$ MeV;

$J^P = \frac{3}{2}^-$: $N(\sim 1520)$, $\Gamma^{\text{tot}} = 105$–$150$ MeV, $\Gamma(\pi N \to \pi N) = 50$–$75$ MeV;

$J^P = \frac{5}{2}^+$: $N(\sim 1688)$, $\Gamma^{\text{tot}} = 105$–$180$ MeV, $\Gamma(\pi N \to \pi N) = 65$–$110$ MeV;

$J^P = \frac{7}{2}^-$: $N(\sim 2190)$, $\Gamma^{\text{tot}} \approx 300$ MeV, $\Gamma(\pi N \to \pi N) \approx 105$ MeV.

The above choices are somewhat arbitrary; if one also assumes that the more weakly coupled $I = \frac{1}{2}$ resonances with $J = l + \frac{1}{2}$ and the $I = \frac{3}{2}$ resonances with $J = l - \frac{1}{2}$ lie on trajectories, then corrections must be made to account for their presence. Note that the Clebsch-Gordan coefficient for πN charge exchange via $I = \frac{1}{2}$ is equal but opposite in sign to that when the reaction goes in an $I = \frac{3}{2}$ state, so that an $I = \frac{1}{2}$ and an $I = \frac{3}{2}$ trajectory with equal intrinsic phases would naturally contribute with opposite sign to the amplitude for the charge-exchange reaction. It is important to note that each trajectory need not have both even- and odd-l values; it is sufficient to have one trajectory with only odd l and another with even l. This means that direct-channel trajectories with $\Delta l = 2$ can contribute to inelastic reactions in the present model as long as two such trajectories contribute, one with even l and one with odd l.

The polarization data of Drobnis *et al.*[17] and Bonamy *et al.*[18] for this reaction were used to fix the amounts of the $J = l \pm \frac{1}{2}$ trajectories more precisely than the differential cross-section data can, and the best fit was obtained for

$$A = 1.2A^+ - A^-, \tag{20}$$

which is similar to the result for $\pi N \to \eta N$ given in

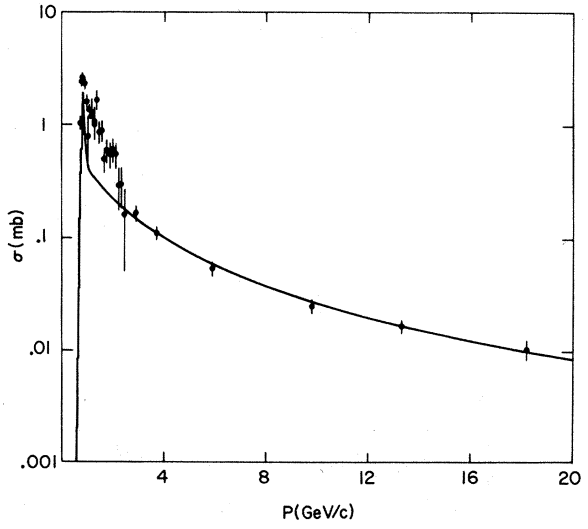

FIG. 5. Cross section for the reaction $\pi N \to \eta N$ vs beam momentum. The data points of Bulos *et al.*, (Ref. 19) span the momentum range from 704 to 1284 MeV/c, those of Danburg (Ref. 14) lie in the interval from 1.14 to 2.46 GeV/c, and those of Guisan *et al.* (Ref. 15) cover the range from 2.91 to 18.2 GeV/c. The curve is from the fit described in the text; it is normalized to pass through the data point at 3.72 GeV/c.

Eq. (18). The high-energy total cross-section data for events in the forward peak of the differential cross section were best described with an exponent in Eq. (15) of $\gamma = 0.1$.

Summarizing the results of the fits to the data in the forward peak of the differential cross section for $\pi^- p \to \pi^0 n$, we have α=200 MeV as the resonance-mass spacing, with the radius of interaction specified by $r = 1.33$ (±10%) in Eq. (17), and $\beta = 400$ MeV as the increase in resonance width for $\Delta l = 1$. The amounts of the assumed dominant $J = l \pm \frac{1}{2}$ trajectories are given by Eq. (20), and $\gamma = 0.1$ is the exponent in Eq. (15). It is emphasized that the resonance spectrum implied by the values of α and β in this fit and for η production are meant to describe the data at high energy. For this reason no particular importance should be attached to the fact that the "smooth" spectra obtained from the fits to the high-energy data do not exactly match the observed baryon spectrum at low energy.

The solid curve in Fig. 6 is the result of the above fit to the forward peak of the differential cross-section data of Sonderegger *et al.*[20]; it is normalized to the area under the forward peak. The dashed curve will be discussed below. In Fig. 7 the polarization data are displayed along with curves from the fit. Figure 8 shows the cross section under the forward peak and the result of the fit; the curve is normalized to pass through the data point at 4.83 GeV/c.

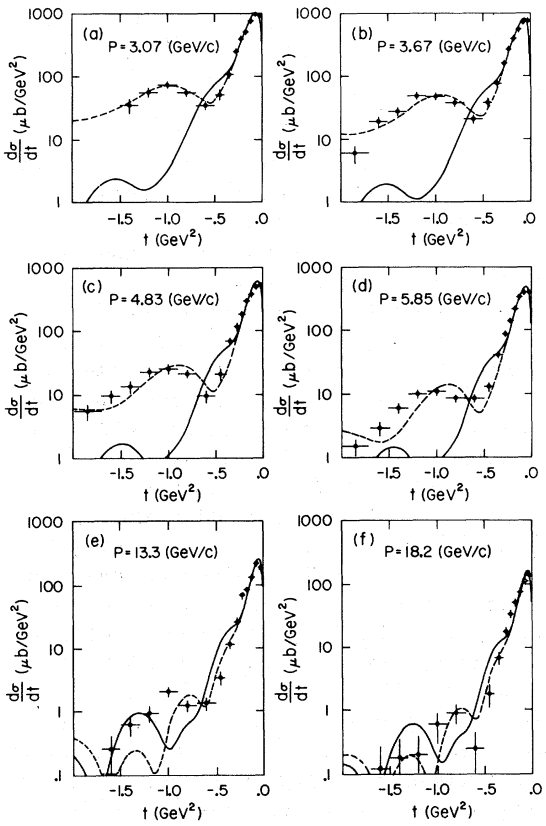

FIG. 6. Differential cross sections for $\pi^- p \to \pi^0 n$ measured by Sonderegger *et al.* (Ref. 20) at six beam momenta. The curves are from the fits described in the text.

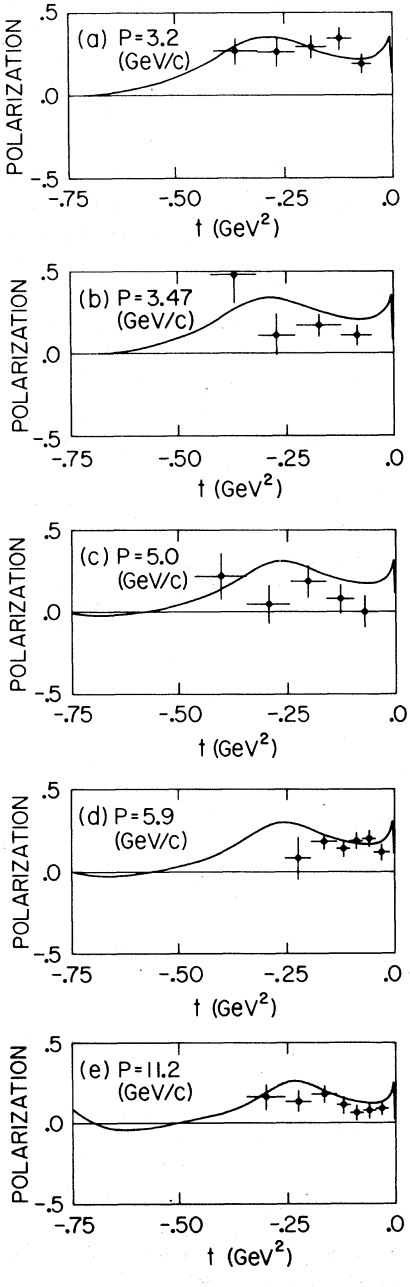

FIG. 7. Polarization in the reaction $\pi^- p \to \pi^0 n$. (a)–(c) from Drobnis *et al.*, Ref. 17; (d)–(e) from Bonamy *et al.*, Ref 18. The curves are from the fit described in the text.

It is evident that the fit described above accounts satisfactorily for the data in the forward peak of the πN charge-exchange differential cross section. As noted above, a fixed-t amplitude like the one given here cannot yield in a simple way the disappearance of the secondary peak in the differential cross section relative to the forward peak. (Note, however, that the shrinkage of the measured forward peak between 3 and 18 GeV/c is followed well by the residual shrinkage of the simple resonance amplitude used here, just as was noted above for the case of η production.) One way to describe the secondary peak is to assume that it is due to the dominantly spin-flip resultant of two or more interfering trajectories. Because the secondary peak is so far from the forward direction (at $t \approx -1$ GeV^2), the resonances on the assumed additional trajectories either must be spaced much more widely than those giving the forward peak, or else r in Eq. (17) is smaller than 1 if the spacing is like that obtained above for the forward peak. The πN coupling to these trajectories then must fall off faster with energy than the coupling to the trajectories giving the forward peak, in order to account for the disappearance of the secondary peak relative to the forward one. There may be other ways of accounting for the behavior of the secondary peak in a suitably refined pure-resonance model, and the procedure suggested here is mentioned only as one possibility.

We will nevertheless show that a rough description of the secondary differential cross-section peak can be achieved in the manner just outlined.

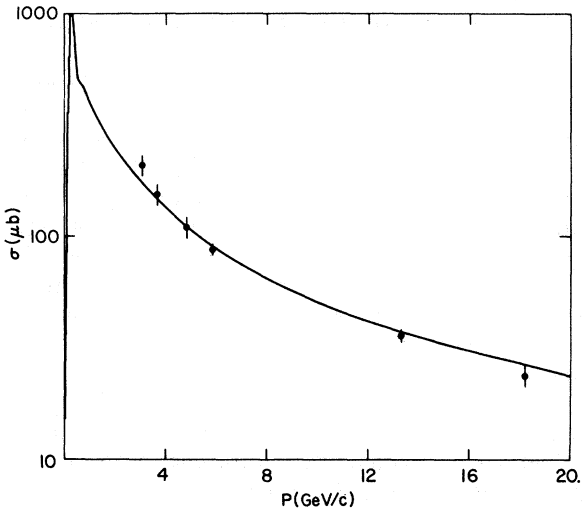

FIG. 8. Cross section for data in the forward peak of the differential cross section in $\pi^- p \to \pi^0 n$ vs beam momentum. The data are from Sonderegger *et al.* (Ref. 20). The curve is from the fit described in the text, normalized to pass through the data point at $p = 4.83$ GeV/c.

The dashed curves in Fig. 6 are the result of an amplitude obtained by adding (with an over-all phase of $-90°$) to the amplitude (20) obtained for the forward peak an amplitude given by

$$A' = A'^{+} - A'^{-}, \tag{21}$$

with $E_l = 1500 + 200l$ MeV as the resonance-mass spectrum, $\Gamma_l^{\text{tot}} = 300 + 400l$ MeV as the resonance-width spectrum, and radius of interaction [see Eq. (17)] $= r = 0.6$. The amount of amplitude (21) relative to amplitude (20) was determined separately at each energy; this relative amount fell off with c.m. energy roughly as E^{-3}, implying $\gamma \cong 3.1$ as the exponent in Eq. (15) appropriate to amplitude A'. It is seen that the addition of this correction term improves the agreement between the curve and the data down to cross-section values about 100 times smaller than those in the forward direction. We note that the addition of the correction amplitude A' affects the polarization predictions shown for the two lowest energies of Fig. 7, but because of the tentative nature of the correction term A', no detailed redetermination of amplitudes (20) and (21) was performed.

DISCUSSION OF RESULTS

It is useful to evaluate the results obtained above and to state what are felt to be the essential as well as the nonessential features of the proposed amplitude.

It has been seen that a simple resonance amplitude, even though constructed with a large number of simplifying assumptions, can satisfactorily account for the main features of two reactions at high energy. In particular, such an amplitude yields roughly the correct polarization observed for the two reactions at high energy.

The essential properties of the amplitude examined here are (a) that resonances are responsible for inelastic two-body reactions, (b) that the highest-spin resonance contributing to a reaction satisfies $J \propto \sqrt{s}$, all higher-spin resonances being damped by angular momentum barrier factors, (c) that the lower partial waves at a given energy are contributed by the high-energy tails of the lower-mass resonances, and (d) that in general two or more direct-channel trajectories contribute to any reaction.

Other features of the amplitude, such as the simple Breit-Wigner line shape and the angular momentum barrier function used [see Eqs. (6) and (13)], are quite arbitrary. It is of great importance to know the correct resonance line shape if the tails of the low-energy resonances are expected to yield the low partial waves at high energy. The choice of the two-body orbital angular momentum

l as the parameter to use in describing the resonance mass and width spectra is also arbitrary; the resonance angular momentum J could just as well be used. Also, Eq. (14) need not describe the baryon spectrum exactly, but may only give the average mass and width increase with l. Because of the several arbitrary features just mentioned, and because of the simplifying assumptions used in performing the fits to the data, the results exhibited here can be considered to be only illustrative of the fits that can be obtained. Furthermore, the presence of more than one resonance in many partial waves in πN scattering indicates that the amplitudes obtained in the fits above should be corrected to account for the presence of more weakly-coupled trajectories other than the assumed dominant two trajectories. In this connection we note also that backward peaks can be generated by trajectories of direct-channel resonances interfering with the proper phase. (See Crittenden *et al.*[8] for a resonance fit to backward π^+p elastic scattering up to $p_{\text{lab}} = 5$ GeV/c using a model different from that proposed here.)

It seems quite important to correlate the resonance spectrum observed at low energy with the scheme proposed here; this was attempted above in connection with the fits to the data for $\pi N \to \eta N$ and $\pi^- p \to \pi^0 n$. It has already been noted in this regard that trajectories with $\Delta J = 2$ can be accommodated if two trajectories contribute, one with odd l and one with even l. This enables a correlation with the trajectories that seem to have $\Delta J = 2$. Another important point is that the proposed spectrum is of the form $E_l \propto l$ instead of the usual form (in terms of Regge theory) $E_l^2 \propto l$. It is interesting to note that it would be difficult to distinguish, at low energy, the observed squared-mass spacing from the linear-mass spacing required by the fits to the high-energy data ($\alpha = \Delta m/\Delta l \approx 200$ MeV). This is because, at $m = 2$ GeV, $\Delta m^2 = 2m\Delta m \approx 0.8$ GeV^2, which is approximately the observed squared-mass spacing. One could even assume a mass spectrum that satisfies $E_l^2 \approx l$ GeV^2 at low energy and $E_l \approx 0.2l$ GeV at high energy; a simple example is $E_l = (l + \frac{1}{25} l^2)^{1/2}$ GeV. The proposed resonance-width spectrum is also consistent with the observed low-spin resonances. Examination of the Particle Data Group listings[16] of baryon resonances shows that resonance widths generally increase with increasing mass (and spin). The broadest resonances listed in the tables have widths up to 450 MeV. It is not implausible to assume that there are baryon resonances broader than 450 MeV; they would not be easily observed simply because of their broadness, especially if their spacing is less than their widths.

Finally, we compare briefly the amplitude given here with other models for two-body scattering. It is interesting to note that this amplitude has just the partial-wave phase behavior of a Regge amplitude, as obtained by Kugler.[2] That is, we have partial waves with nonresonant behavior [Eq. (7)] for $l \ll \sqrt{s}$ and resonant behavior [imaginary amplitude, as given by Eq. (8)] for $l \sim \sqrt{s}$. Kugler also finds the widths of the resonances in the highest partial waves to be proportional to $\sqrt{s}$, as is postulated here. The agreement between the simple model given here and the partial-wave behavior of a Regge amplitude is perhaps a coincidence; Collins, Johnson, and Squires,[22] and Chiu and Kotański[23] have questioned the resonance interpretation of the Argand-diagram loops generated by a Regge amplitude. There is a more important difference between the simple amplitude constructed above and a Regge amplitude: A Regge amplitude has the asymptotic behavior $s^{\alpha(t)}$, whereas the present amplitude is constructed to give, for large s, a constant-width (nonshrinking) t distribution; it can only be compared with a Regge amplitude in the special case $\alpha(t) = \text{constant}$ for $t < 0$. This is not an accident; Mandula and Slansky[24] have shown that an amplitude constructed from one trajectory of direct-channel resonances, as is proposed here, *cannot* exhibit Regge asymptotic behavior.

The difference between the above property (c) of the present amplitude and the Veneziano model is important; in the Veneziano model the lower partial waves are assumed to come from daughter states at the same mass. The apparent absence of the required great number of daughter states is a difficulty of the Veneziano model.[25]

The above-mentioned articles by Hoff[9] and Dikmen[10] correlating structure in the $\pi^- p$ elastic differential cross section with direct-channel resonances employed only a finite number of resonances and were applied only up to moderate energies. In the more recent work of Dikmen[6,7] in describing elastic scattering, resonance contributions are included only up to $p_{\text{lab}} \approx 6$ GeV/c; furthermore these resonances are assumed to lie on trajectories with $E_l^2 \propto l$. In the present paper we have investigated the general conditions under which resonances might account for peripheral inelastic meson-baryon scattering at all energies.

The work of Crittenden *et al.*[8] in describing $\pi^+ p$ backward elastic scattering using resonance contributions embodies a very different approach from the one described here. A number of assumptions differ from those in this paper; the crucial difference between the two methods is that Crittenden *et al.* use a resonance line shape which is made to disappear at energies more than one full width away from the resonance mass, whereas here a continuous line shape is assumed.

ACKNOWLEDGMENTS

The author is grateful to Dr. Donald W. Davies, Dr. Geoffrey Fox, Dr. George R. Kalbfleisch, Dr. Janos Kirz, and Dr. Richard C. Slansky for valuable criticisms and helpful discussions.

---

*Work performed under the auspices of the U. S. Atomic Energy Commission.

[1]C. Schmid, Phys. Rev. Letters 20, 689 (1968).
[2]M. Kugler, Phys. Rev. Letters 21, 570 (1968).
[3]H. Harari, Phys. Rev. Letters 20, 1395 (1968).
[4]H. Harari, in 1969 Brookhaven Summer School Lectures, BNL Report No. 50212 (C-58) (unpublished).
[5]J. A. Shapiro, Phys. Rev. 179, 1345 (1969).
[6]F. N. Dikmen, Phys. Rev. Letters 22, 622 (1969).
[7]F. N. Dikmen, Lett. Nuovo Cimento 1, 544 (1969).
[8]R. R. Crittenden, R. M. Heinz, D. B. Lichtenberg, and E. Predazzi, Phys. Rev. D 1, 169 (1970).
[9]G. T. Hoff, Phys. Rev. Letters 18, 816 (1967).
[10]F. N. Dikmen, Phys. Rev. Letters 18, 798 (1967).
[11]D. R. O. Morrison, Phys. Letters 22, 528 (1966).
[12]R. Dolen, D. Horn, and C. Schmid, Phys. Rev. 166, 1768 (1968).

[13]Note that at high energy $k_l = \frac{1}{2}E_l$, and thus $k_l \propto \Gamma_l$ with the assumptions used here. Now $\Gamma_l \propto R_l^{-1}$, where R_l is the spatial size of each resonance; this size can be taken to be the radius of interaction, so that the factors of k/k_l can be written in the familiar form kR_l. Further note that if the factors of k/k_l are replaced by the general form rk/k_l, where r is a constant, then the sum of partial waves will cut off when $E \approx E_l/r \approx \alpha l/r$. The effective diffraction radius then becomes $R = 2r/\alpha$ [cf. Eq. (5)].

[14]J. S. Danburg, Ph. D. thesis, LRL Report No. UCRL-19275, 1969 (unpublished); J. S. Danburg *et al.*, Phys. Rev. D 2, 2564 (1970).
[15]O. Guisan *et al.*, Phys. Letters 18, 200 (1965).
[16]Particle Data Group, Rev. Mod. Phys. 42, 87 (1970).
[17]D. D. Drobnis *et al.*, Phys. Rev. Letters 20, 274 (1968).
[18]P. Bonamy *et al.*, Nucl. Phys. B16, 335 (1970).
[19]F. Bulos *et al.*, Phys. Rev. Letters 13, 486 (1964).
[20]P. Sonderegger *et al.*, Phys. Letters 20, 75 (1966).
[21]A. Donnachie, R. G. Kirsopp, and C. Lovelace, Phys. Letters 26B, 161 (1968).
[22]P. D. B. Collins, R. C. Johnson, and E. J. Squires, Phys. Letters 27B, 23 (1968).
[23]C. B. Chiu and A. Kotański, Nucl. Phys. B7, 615 (1968).
[24]J. E. Mandula and R. C. Slansky, Phys. Rev. Letters 20, 1402 (1968).

[25]I am grateful to G. C. Fox for emphasizing these points (private communication).